Maternal diet and gut microbiome composition modulate early life immune responses

Erica T. Grant[1,2], Marie Boudaud[1], Arnaud Muller[3,4], Andrew J. Macpherson[5], and Mahesh S. Desai[1,6,*]

[1]Department of Infection and Immunity, Luxembourg Institute of Health, Esch-sur-Alzette, Luxembourg

[2]Faculty of Science, Technology and Medicine, University of Luxembourg, Esch-sur-Alzette, Luxembourg

[3]Bioinformatics Platform, Data Integration and Analysis, Luxembourg Institute of Health, Strassen, Luxembourg

[4]LuxGen, Translational Medicine Operation Hub, Luxembourg Institute of Health, Dudelange, Luxembourg

[5]Department of Visceral Surgery and Medicine, Bern University Hospital, University of Bern, 3010, Bern, Switzerland.

[6]Odense Research Center for Anaphylaxis, Department of Dermatology and Allergy Center, Odense University Hospital, University of Southern Denmark, Odense, Denmark

*Correspondence: mahesh.desai@lih.lu

Abstract

In early life, the intestinal mucosa and immune system undergo a critical developmental process to contain the expanding gut microbiome while promoting tolerance towards commensals, yet the influence of maternal diet and gut microbial composition on offspring immune maturation remains poorly understood. We colonized gnotobiotic mice with a defined consortium of 14 strains, fed them a fiber-free diet, and then longitudinally assessed offspring development during the weaning period. Unlike pups born to dams fed a standard, fiber-rich chow, pups of fiber-deprived dams demonstrated delayed colonization with *Akkermansia muciniphila*, a mucin-foraging bacterium that can also utilize milk oligosaccharides. The pups of fiber-deprived dams exhibited an enrichment of colonic tissue transcripts corresponding to defense response pathways and a peak in *Il22* expression at weaning. Removal of *A. muciniphila* from the community, but maintenance on the fiber-rich diet, was associated with reduced proportions of RORγt-positive innate and adaptive immune cell subsets. Our results highlight the potent influence of maternal dietary fiber intake and discrete changes in microbial composition on the postnatal microbiome assemblage and early immune priming.

Introduction

Dietary fiber plays a major role in shaping the colonic gut microbiome and host immunity, however the impact of maternal dietary fiber intake on the offspring's microbiome and immune development is largely associative for the early life period (Mirpuri, 2021). In adult mice, dietary fiber deprivation leads to microbiome-driven thinning of the mucus layer, which can increase susceptibility to a range of conditions including enteric pathogen infection (Desai *et al*, 2016; Neumann *et al*, 2021), graft-versus-host disease (Hayase *et al*, 2022), and food allergy (Parrish *et al*, 2022a). Although exposure to microbial metabolites in utero initiates innate immune responses and barrier development in pups (De Agüero *et al*, 2016), the postnatal period is also critical for healthy maturation of intestinal function and adaptive immunity in a complex process that is partially driven by a response to the colonizing microbiome (Kalbermatter *et al*, 2021; Wells *et al*, 2022). In particular, from 2–4 weeks of age, mouse pups transition from breast milk to solid food with an accompanying shift in microbial composition and a vigorous immune response to the expanding microbiota (Al Nabhani *et al*, 2019). Without this "weaning reaction", as observed in germ-free and broad-spectrum antibiotic-treated mice, Al Nabhani *et al* reported increased susceptibility to inflammatory pathologies (Al Nabhani *et al*, 2019). However, it remains unclear how variations in the maternal diet or defined differences in microbial composition affect early life immune priming (Ansaldo *et al*, 2021).

We therefore set out to investigate the influence of maternal dietary fiber intake on the offspring colonic development by feeding dams either a standard fiber-rich (FR) chow or a custom fiber-free (FF) diet (Desai *et al*, 2016) (**Fig. 1a**). To standardize the bacterial composition and facilitate interpretation of the microbial shifts, we utilized a gnotobiotic mouse model consisting of 14 bacterial strains (14-member synthetic human gut microbiota or 14SM) that form a functionally diverse community (Desai *et al*, 2016; Steimle *et al*, 2021). Although this community was designed to resemble an adult microbiota, one member— *Akkermansia muciniphila*—is capable of degrading milk oligosaccharides and is an early colonizer of the gut (Kostopoulos *et al*, 2020). This taxon is also enriched under fiber-deprived conditions in adult mice (Desai *et al*, 2016) and appears to have

immunogenic properties when present in 14SM, including a high IgA-coating index (Pereira *et al*, 2022). We sought to determine the role of this particular microbe in early life development on the same FR diet by employing mice colonized with the full community except *A. muciniphila* (13SM). By employing a longitudinal sampling approach among the pups of each diet and SM combination, we isolated dietary and microbial drivers of early-life immune development. We show that, while maternal diet had a strong impact on the host epithelial transcriptome, the presence or absence of *A. muciniphila* was a key contributing factor in shaping immune cell differentiation during this critical early life window.

Results and discussion

Gut microbiome colonization is shaped by maternal diet

Consistent with previous reports (Earle *et al*, 2015; Desai *et al*, 2016), we observed an elevated relative abundance of *Akkermansia muciniphila* in the parent mice fed a fiber-free (FF) diet compared to those on a standard fiber-rich (FR) chow (**Table S2**). We expected to observe similarly high levels of *A. muciniphila* in the offspring of FF-fed dams; however, the expansion of *A. muciniphila* was delayed among mice born to FF-fed dams (**Fig. 1A–C)**. This contrasts with the microbiome development of 14SM FR pups, which showed strong initial colonization with *A. muciniphila* during suckling, as anticipated given its ability to consume milk oligosaccharides (Kostopoulos *et al*, 2020). When mice began to consume a solid food diet between ages 15 to 20 days, the profiles rapidly stabilized and resembled compositions observed in adult mice fed the respective diets (**Table S2, S3**). Among 14SM FF mice, *A. muciniphila* (mucin specialist), *Bacteroides caccae* (mucin generalist), *Clostridium symbiosum* (an emerging biomarker for colorectal cancer (Xie *et al*, 2017)), and *Desulfovibrio piger* (sulfate reducer) significantly expanded to comprise approximately three-fourths of the microbiome composition.

Colonic transcriptome reflects differences in maternal diet

A. muciniphila has been previously associated with regulation of host metabolic activity (Yoon *et al*, 2021) and intestinal adaptive immunity in adult mice (Ansaldo *et al*, 2019), but little is known about its immune influence in early life. Therefore, to address the host physiological effects of this striking difference in the abundance of *A. muciniphila* according to diet (**Fig. 1**), we performed total RNA sequencing on colon of 15 day-old pups born to FR and FF 14SM dams as well as FR 13SM dams without *A. muciniphila* (**Fig. 2**). Relative to the control group (14SM FR), we detected changes in the expression level of 32 transcripts according to the maternal diet (14SM FF) and 57 transcripts regulated by the presence of *A. muciniphila* (13SM FR) (**Fig. 2A upper table, Fig. 2B**, **Fig. S1B)**. Performing a pathway level analysis based on Gene Ontology (GO) terms for biological processes, we found differential enrichment according to the diet (14SM FR vs 14SM FF), but not to the presence of *A. muciniphila* (14SM FR vs 13SM FR) (**Fig. 2A, lower table**). Comparing host transcriptomes according to diet revealed an enrichment in FF 14SM pups of transcripts involved in epithelial barrier development and cell–cell adhesion (*Myh1*, *Myh8*, and *Myot*), as well as peptide cross-linking (*Sprr1a* and *F13a1*), anoikis or apoptosis associated with cell detachment from the epithelial tissue (*Clca3a2* and *Itga5*), oxidative stress-induced intrinsic apoptotic signaling pathways (*Hspb1* and *Nox1*), and response to interferon-beta (*Tgtp2*, *Gbp2* and *Igtp*) (**Fig 2B and B, Table S8**). Some of these transcripts, including *Nox1* (Szanto *et al*, 2005), *Itga5* (Zhu *et al*, 2021), and *Hspb1* (Arrigo *et al*, 2007), are also implicated in colon cancer progression, suggesting potential pathological development.

The postnatal period is critical for the development of the immune system as a weaning reaction to colonizing microbes was shown to be protective against diseases in adulthood among mice colonized with segmented filamentous bacteria (Al Nabhani *et al*, 2019). Thus, in order to provide a longitudinal element to the transcriptomic data, we performed RT-qPCR to quantify the relative expression of transcripts corresponding to select cytokines involved in immunity and epithelial barrier maintenance (**Fig. 2D**). We noted an induction of *Infg* around 15 days among all groups, which is considered characteristic of the weaning reaction. *Tnfa*, another marker of the weaning reaction,

was only elevated in the pups of 14SM fiber-deprived dams. By comparing transcript expression levels to germ-free (GF) mice at age 15 days (**Fig. 2D**), we see that some of the observed pro-inflammatory shifts can be attributed to a combination of diet and microbiome composition. In particular, at age 15 days, the FF diet increased the transcript levels of *Ifng*, *Il17f*, and *Il23* among germ-free pups of fiber-deprived dams, relative to germ-free, fiber-rich-fed offspring (**Fig. 2D, Fig. S1C**). At the same age, only pups of 14SM FF-fed dams displayed a strong elevation in *Tnfa* and *Il22* transcript levels, reflecting compounding effects of the maternal diet and microbiome.

Immune development due to maternal fiber deprivation modified by microbiota

The transcript-level results underscore the potent impact of the maternal diet in shaping the developing epithelial barrier and host immune system. Therefore, to confirm that these changes translate into the profile of immune cell populations, we performed flow cytometry on cells isolated from the colonic lamina propria (cLP) at age 15 days (**Fig. 3, Fig. S2**). As an effect of colonization, we observed elevated levels of NK cells and ILC3 among 14SM pups compared to GF pups (**Fig. 3A**). Consistent with the host transcriptomic data, maternal dietary fiber intake appeared to play a role in immune cell profiles of both 14SM and GF pups. Particularly, pups of 14SM FF dams had lower levels of ILC2 and higher levels of ILC3 NCR^- compared to pups of 14SM FR dams (**Fig. 3A**). In the adaptive arm however, the 14SM colonization lowered the proportions of $CD8^+$, $CD4^+$, Tregs and Th1 cells (**Fig. 3B**). By contrast, Th17 cells were induced by the colonization but lower among pups of fiber-deprived dams, suggesting that the maternal dietary fiber intake differentially affects innate and adaptive $RORgt^+$ cells in the pup's colons.

Given that a trend toward ILC3 induction was also observed in GF pups of dams fed the FF diet, relative to the GF FR group, it is also possible that dietary metabolites other than bacterially produced SCFA play a role in shaping host immunity. In particular, even in the absence of a microbiota, AhR activation through the binding of these metabolites might promote epithelial protection via ILC3 rather than ILC2 induction (Qiu *et al*, 2012; Li *et al*, 2018). AhR ligands, which may be derived from

microbial or host degradation of dietary tryptophan metabolites, stimulate production of IL-22 from ILC3s (Qiu *et al*, 2012; Li *et al*, 2018), both of which were elevated among pups of 14SM FF-fed dams at 15 days of age. The expansion of these innate subsets also leads to apoptosis of commensal-specific CD4+ and CD8+ T cells (Hepworth *et al*, 2015; Liu *et al*, 2019). A fixed number of cells were stained per organ, therefore, although GF mice have higher proportions of adaptive cell subsets (namely CD8+, CD4+, Tregs, and Th1 cells), this is likely a reflection of their lower proportions of innate cells, consistent with previous reports (Macpherson & Harris, 2004; Kennedy *et al*, 2018). The absolute counts of regulatory T cells are expected to be lower in GF mice compared to colonized mice (Macpherson & Harris, 2004; Hrncir *et al*, 2008).

Akkermansia muciniphila *alters innate and adaptive immunity in early life*

To determine the role of *A. muciniphila* in the aforementioned colonization effect (**Fig. 3A, B**), we compared the immune cell profiles of pups born to FR-fed 14SM, 13SM and GF dams (**Fig. 3C, D**). Compared to GF pups, the pups born to mothers without *A. muciniphila* (13SM) had lower induction of ILC3 and Th17 cells, and lower repression of CD8+, CD4+, Tregs, Th1 and Th2 cells (p=0.052) than pups born to 14SM dams (**Fig 3C, D**). Interestingly, the group with the highest levels of *A. muciniphila* at this time point (14SM FR) also had an enrichment of Th17 cells (**Fig. 3D**). Th17 cells play a key role in progression of multiple sclerosis, an autoimmune disease that has also been correlatively linked to presence of *A. muciniphila* in patients (Jangi *et al*, 2016) and mechanistically in mouse models of multiple sclerosis (Lin *et al*, 2021). Although the precise nature of the link between *Akkermansia* and exacerbation of autoimmune encephalomyelitis has not yet been shown (e.g. MAMP recognition, physiological alterations from mucin-degrading activities), this relationship bears further investigation to identify potential therapeutic targets.

Conclusion

Summarizing these findings, we demonstrate 1) that the maternal diet alters the host transcriptomic profile among pups during the weaning period and 2) that the inclusion or exclusion of a single

bacterium from a defined community has demonstrable effects on the immune development of the pups (**Fig. 4**). The mechanisms behind such immunomodulatory effects can be via microbial metabolites such as SCFA or AhR ligands, or via surface molecules such as LPS (Davis *et al*, 2022). In the latter instance, Kostopoulos et al. demonstrated that *A. muciniphila* produces more immune-regulatory pili-protein when grown on human milk, highlighting diet-dependent factors that can indirectly strengthen barrier integrity via the microbiome (Kostopoulos *et al*, 2020). In line with this, we found that presence of *A. muciniphila* skews toward a type 3 response, whereas its absence appears to favor a type 1 or 2 response. Overall, our results highlight the importance of the maternal microbiome composition and dietary fiber intake in postnatal microbiome maturation and immune development, which could have implications for development of various immune-mediated diseases later in life.

In this study, we assessed the compounding effects of a fiber-free diet across generations with mice pups weaned onto the same diet as the dams. While this experimental setup more closely resembles a real-world scenario, future studies could isolate the effects of the maternal fiber-deprived diet alone by weaning mice onto the same standard chow. Furthermore, we note that it would be of interest to interrogate the long-term health consequences of the observed differences in early life immune priming (**Fig. 4**). Mouse models of multiple sclerosis or allergy might be particularly interesting based on the immune cell subsets that were strongly affected by the maternal diet or microbiome changes in this experiment.

Additionally, future studies should characterize the maternal milk components improve understanding of the mechanisms for *A. muciniphila* suppression, which occurred only in pups born to fiber-deprived dams. As illustrated in **Fig. 4**, a potential explanation for this phenomenon includes changes in quantity or specificity of IgG—the dominant maternal antibody transferred via murine breast milk (Zheng *et al*, 2020). In adult mice, this role is carried out by IgA, which can regulate the composition and metabolic output of the gut microbiome (Nakajima *et al*, 2018). Another explanation

for *A. muciniphila* suppression may be related to differences in the types of linkages presented by the milk oligosaccharides, which could hamper their effective utilization by *A. muciniphila.* To this point, Kostopoulos et al. demonstrated that *A. muciniphila* can degrade 2'-fucosyllactose, lacto-N-tetraose, lacto-N-triose II, lactose, and 3'-sialyllactoses (Kostopoulos *et al*, 2020), although it also bears mentioning that these structures are common components of human milk, which is expected to have a slightly different compositional and structural makeup compared to murine milk (Luna *et al*, 2022). Improved understanding of these milk-associated mechanisms in both humans and rodent models are warranted, as these insights could provide tools to augment growth or activity of *A. muciniphila* in various disease contexts.

This work highlights numerous underexplored factors related to the potential for maternal fiber deprivation to alter postnatal establishment of mucin-degrading gut bacteria and immune maturation. The elevated levels of RORgt-induced innate and adaptive cell subsets among *A. muciniphila*-colonized mice is important for preventing translocation of gut microbes into the host (De Agüero *et al*, 2016) and can also be associated with protection against chronic inflammation via TLR4 (Liu *et al*, 2022). Considering *A. muciniphila* is only found in approximately half of the human population (Geerlings *et al*, 2018), linking this bacterium to exacerbation or amelioration of specific gut-linked diseases is particularly interesting as it highlights its potential as a biomarker for disease risk. Although *A. muciniphila* has been proposed as a probiotic (Cheng & Xie, 2021), mainly due to its strong benefits in countering metabolic diseases, the various conflicting reports involving this bacterium and health, as discussed by Cirstea et al. (Cirstea *et al*, 2018), caution against premature generalizations and underscore the need to consider factors such as diet and underlying disease context. Ultimately, insights provided by the present study and follow-up works are expected to hold translational relevance in improving human health outcomes as modern lifestyle practices (e.g. antibiotics use, Western-style diets) contribute to perturbation of the gut microbiota and immune function across generations (Sonnenburg *et al*, 2016) and in early life (Robertson *et al*, 2019).

Materials and Methods

Mice

All experimental procedures involving animals (i.e. initial gavage of parental mice) were approved by the Luxembourgish Ministry of Agriculture, Viticulture and Rural Development (LUPA 2019/49). Mouse work was performed according to the “Règlement grand-ducal du 11 janvier 2013 relatif à la protection des animaux utilisés à des fins scientifiques” based on the “Directive 2010/63/EU” on the protection of animals used for scientific purposes. Mice were housed in the germ-free facility of the University of Luxembourg in either colonization-specific isolators or individually ventilated cages. Germ-free Swiss Webster mice were orally gavaged with 13SM or 14SM at 6–8 weeks of age. Gnotobiotic mice and germ-free (GF) controls were fed the respective diets for at least 20 days prior to start of breeding. Mouse pups between ages 10–30 days were sacked by decapitation (age 10 days) or cervical dislocation (age >15 days) at 5-day intervals to collect endpoint measures.

Diet formulation

Detailed compositions of the fiber-rich (FR) and fiber-free (FF) diets used in this study are as previously reported (Parrish *et al*, 2022c). Gnotobiotic FR mice were fed a standard rodent chow (SAFE®R04, Augy, France). The FF diet is a modified version of Harlan TD.08810 diet, manufactured by the same vendor as the standard chow, as previously reported(Parrish *et al*, 2022b).

Bacterial culturing and colonization of 13- or 14-member synthetic microbiota (SM)

Culturing and colonization of GF mice with the 13- or 14-member synthetic microbiota (SM) was performed as previously described (Steimle *et al*, 2021). The 14SM community contains the following bacteria (all type strains, unless otherwise indicated): *Akkermansia muciniphila*, *Collinsella aerofaciens*, *Desulfovibrio piger*, *Escherichia coli* HS, *Faecalibacterium prausnitzii* A2-165, *Roseburia intestinalis*, *Marvinbryantia formatexigens*, *Clostridium symbiosum*, *Eubacterium rectale* A1-86, *Barnesiella intestinihominis*, *Bacteroides caccae*, *Bacteroides uniformis*, *Bacteroides ovatus*,

and *Bacteroides thetaiotaomicron*. The 13SM mice were orally gavaged with the same strains with the exception of *A. muciniphila*. Bacterial colonization among the parental mice was verified by qPCR of fecal DNA at 7 days post-oral gavage using strain-specific primers. Note that *R. intestinalis* and *E. rectale* did not consistently transfer to the pups during the early life period, despite being detected in the parents.

Tissue processing

Distal colons were washed in PBS to collect contents, then transferred to 1 ml RNAprotect Tissue Reagent (Qiagen, Hilden, Germany) for transcript analyses. Tissues were held in RNAprotect at 4°C for 2 days, after which the reagent was removed and the tissues stored at –80°C. For mice that would undergo FACS analyses, the entire colon was transferred into ice-cold 3 ml Hank's balanced salt solution (HBSS) containing 10 mM HEPES and without Ca^{2+} and Mg^{2+}. Cells from the colonic lamina propria (cLP) were isolated using a Lamina Propria Dissociation Kit (Miltenyi Biotec, Bergisch Gladbach, Germany) on the gentleMACS Dissociator (Miltenyi Biotec), following the manufacturer's instructions. Cells were washed, counted, and re-suspended in FACS buffer (PBS; 1% FCS; 5mM EDTA) until cell staining.

Flow cytometry

A total of 1.5×10^6 cells per animal were transferred into a U-bottom 96-well plate for staining. For live/dead staining, cells were incubated in 100 µl PBS 1X containing 1.5 µL Zombie NIR Fixable Viability kit (BioLegend, San Diego, CA, USA) at 4°C for 30 min. Cells were washed twice using FACS buffer and subsequently fixed with the FoxP3 Fix/Perm kit (eBiosciences, Uithoorn, Netherlands) for 45 min at 4°C, followed by permeabilization wash. Purified Rat Anti-Mouse CD16/CD32 (Mouse BD Fc Block™, BD Biosciences, San Jose, CA, USA) was added at a concentration of 1 µg per 10^6 cells, incubated at 4°C for 30 min, then cells were washed twice in permeabilization buffer. Cells were stained with anti-CD4 BV605 (#100548, clone RM4-5, 1:700, Biolegend), anti-CD3 BV711 (#100241, clone 17A2, 1:88, Biolegend), anti-CD45 BV780 (#564225,

clone 30-F11, 1:88, BD), anti-CD335/NKp46 FITC (#137606, clone 29A1.4, 1:100, Biolegend), anti-CD8 PE-Cy5 (#100710, clone 53-6.7, 1:700, Biolegend), anti-FoxP3 eF450 (#48-5773-82, clone FJK-16s, 1:200, eBiosciences), anti-GATA3 PE (#100710, clone 53-6.7, 1:44, Biolegend), anti-EOMES PE-eF610 (#61-4875-82, clone Dan11mag, 1:100, eBiosciences), anti-Tbet PE-Cy7 (#644824, clone 4B10, 1:44, Biolegend), and anti-RORgt APC (#17-6988-82, clone AFKJS-9, 1:22, eBiosciences). Cells were incubated with the staining mix for 30 min at 4°C, then washed twice with FACS buffer. Samples were acquired on a NovoCyte Quanteon flow cytometer (ACEA Biosciences Inc., San Diego, CA, USA). Raw fcs files were analyzed in FlowJo version 10.8.1, with innate cell populations gated as described by Burrows et al. (Burrows *et al*, 2020). An example of the gating strategy is illustrated in **Fig. S2**. The dataset was exported as a percent of the total $CD45^+$ cells for subsequent statistical analyses.

DNA extraction and microbiome compositional analyses

Distal colon contents were collected by opening the colon longitudinally and washing tissue in 1 ml PBS. The PBS and contents were then centrifuged at 10 000 g for 10 min and the PBS supernatant was removed. Pelleted contents were stored at –20°C until DNA extraction using the phenol-chloroform method, as described by Steimle et al. (Steimle *et al*, 2021). The concentration of DNA was measured using a NanoPhotometer N60 (Implen, Munich, Germany). The purified DNA was diluted 10-fold and then subjected to qPCR with primers specific to each of the 14 bacterial strains, as previously described (Steimle *et al*, 2021). As the primers are specific to each strain and the target sequence is present only once in the respective genome (Desai *et al*, 2016), this method was used to allow for estimation of the number of each individual bacterial genomes or the absolute abundance of bacteria in the contents of the distal colon (**Table S2, S3**). In order to rule out contamination with non-14SM strains, we also performed 16S sequencing on a subset of samples. For this method, DNA concentration was assessed using the Qubit® dsDNA HS assay kit on a Qubit® 3.0 fluorometer (Life Technologies, Eugene, Oregon, USA). To rule out contamination with non-14SM members, sequencing of the V4 region of the 16S rRNA gene was carried out on an Illumina MiSeq system at

the Integrated BioBank of Luxembourg (IBBL, Dudelange, Luxembourg), as previously described by Neumann et al. (Neumann *et al*, 2021). Raw fastq sequences were processed via QIIME2 version 2020.6 (Bolyen *et al*, 2019) using DADA2 (Callahan *et al*, 2016) for quality control. Taxonomic assignment was carried out with the SILVA 138 database (Quast *et al*, 2013) (**Table S4**).

RNA extraction

Colon tissues were stored at –80°C until RNA extraction. Tissues were incubated overnight at –80°C in 1 ml TRIzol™ Reagent (Life Technologies Europe BV, Bleiswijk, Netherlands). A 5mm autoclaved metal bead was added to the sample, followed by homogenization on a RETSCH Mixer Mill MM 400 for 5 min at 30 Hz. Samples were centrifuged at 4°C for 5 min at 12 000 × g. The supernatant was transferred to a new tube and incubated for 5 min at room temperature. For each sample, 200 µl pure chloroform was added, then mixed by shaking for 15 s and incubated at room temperature for 3 min. Next, samples were centrifuged for 15 min at 4°C, 12 000 × g, and the aqueous phase was recovered. A volume of 500 µl isopropanol was added, followed by vigorous mixing and incubation at room temperature for 10 min. Samples were centrifuged at the same settings as previously. Then, the pellet was recovered and washed in 1 ml ice-cold 75% ethanol and vortexed briefly before centrifugation at 4°C for 5 min at 7 500 × g. The supernatant was discarded and the pellets were air-dried for 10 min at 37°C before re-suspending in 50 µl Invitrogen™ UltraPure™ DNase/RNase-free distilled water (Life Technologies Europe BV, Bleiswijk, Netherlands). The RNA solution was further incubated for 15 min at 56°C to fully re-suspend the pellet. DNase treatment to remove genomic DNA was done by adding 2 µl DNAse I (1 U/µl), 10 µl DNase I Buffer (10X), plus 40 µl water for 30 min at 37°C. Next, 1 µl of 0.5M EDTA was added to each sample and the DNAse I was inactivated by heating at 65°C for 10 min. RNA purification was performed with the RNeasy mini kit (QIAGEN Benelux BV, Venlo, Netherlands) according to manufacturer's instructions. RNA was eluted in Invitrogen™ UltraPure™ DNase/RNase-free distilled water (Life Technologies Europe BV, Bleiswijk, Netherlands) and stored at –80°C.

RT-qPCR

Complementary DNA libraries were prepared from 2000 ng purified RNA in 11 µl water, 1 µl 2.5 uM random primers and µl 500 uM dNTPs (Life Technologies Europe BV, Bleiswijk, Netherlands), heated to 65°C for 5 min (lid temperature 112°C), then incubated at 4°C for at least 1 min. Afterwards, 1x SSIV buffer, 1 µl DTT, 1 uL RNaseOUT, and 1 uL SuperScript™ IV Reverse Transcriptase (Life Technologies Europe BV, Bleiswijk, Netherlands) was added to each tube. Samples were held at 23°C for 10 min, then 50°C for 10 min, and finally heated to 80°C for 10 min to inactivate enzymes. Quantitative PCR was carried out according to standard protocols, briefly: 1 ul of template cDNA was mixed with 8.7 µl water,1.2 µl 1x buffer, 0.625 µl 2.5 mM MgCl2, 0.5 µl 400uM dNTPs, 0.1 µl each of 0.2 uM forward and reverse primers (**Table S1**), 0.125 µl 1x SYBR green fluorescent dye, and 0.1 µl 0.5 U Taq DNA polymerase (Life Technologies Europe BV, Bleiswijk, Netherlands). Samples were pre-denatured at 94°C for 5 min; then underwent 40 cycles at 94°C for 20 s, 60°C for 50 s, 72°C for 45 s. Finally, samples were maintained at 72°C for 5 min and the melting curve was generated over 15 s by heating from 65°C–95°C at 0.3°C increments. Transcript expression levels were normalized to levels of *Hprt*, which was identified as the most stable housekeeping gene over time and conditions using RefFinder, in comparison to *Gapdh* and *Hsp90*.

RNA sequencing and analysis

RNA integrity (RIN) was determined using a 2100 Bioanalyzer RNA Nanochip (Agilent, Santa Clara, CA, USA). Samples selected for RNA sequencing had RIN values ranging from 7.7–9.8. RNA libraries were prepared using an Illumina® Stranded Total RNA Prep kit, along with Ribo-Zero Plus to deplete ribosomal RNA. Samples were then sequenced in a 2 × 75 bp arrangement with a High Output Flow Cell on an Illumina NextSeq 550 system (Illumina, San Diego, CA, USA) at the LuxGen sequencing platform (Dudelange, Luxembourg). Adapters were removed using Cutadapt (Martin, 2011), followed by reads mapping and enumeration of gene counts with STAR 2.7.9a (Dobin *et al*, 2013) (**Table S5**). Transcripts that did not appear at least one time on average across all samples were filtered from downstream analyses. Two outliers were identified based on variation on PC1

from the top 500 most variable genes and excluded from subsequent analyses (**Fig. S1a**). Samples normalization was performed using the median of ratios method, followed by differential expression analysis in R using DESeq2 1.30.1 (Love *et al*, 2014). Default parameters were used and *p* values were adjusted according to the Benjamini-Hochberg method. Differential expression was considered significant based on an adjusted *p* value<0.05. Differential expression analysis was performed for pairwise comparisons 14SM FF vs 14SM FR (**Table S6**) and 14SM FR and 13SM FR (**Table S7**) (Love *et al*, 2014). Pathway-level analysis was also carried out in R using the clusterProfiler 3.18.1 enrichGO function (Yu *et al*, 2012) to identify up- or downregulated pathways according to Gene Ontology (GO) terms (**Table S8**).

Statistical analysis

Unless otherwise specified, statistical analyses were carried out using GraphPad Prism version 9.3.1 for Windows (GraphPad Software, San Diego, CA, USA). For FACS data with only one time point, an ordinary two-way ANOVA was fitted to main effects only (diet and colonization status) with multiple comparison correction using the Benjamini-Hochberg method. Only biologically-relevant pairwise statistical comparisons are shown: 13SM FR vs. 14SM FR, 13SM FR vs. GF FR, 14SM FR vs. 14SM FF, 14SM FR vs. GF FR, 14SM FF vs. GF FF, and GF FR vs. GF FF. Data are from independent experiments (pups born from up to 4 litters derived from 2–3 breeding pairs per condition).

Data Availability

The datasets produced in this study are available in the following databases:

- RNA-Seq and 16S rDNA data: European Nucleotide Archive (ENA) at EMBL-EBI PRJEB55622 (https://www.ebi.ac.uk/ena/browser/view/PRJEB55622)
- Flow cytometry data: FlowRepository (Spidlen *et al*, 2012) FR-FCM-Z5X6 (https://flowrepository.org/id/FR-FCM-Z5X6)

Acknowledgements

Figure 4 was made using BioRender (Biorender.com). We thank the Luxembourg National Research Fund (FNR) for funding this research through CORE grants (C15/BM/10318186 and C18/BM/12585940) to M.S.D.; E.T.G. was supported by the FNR PRIDE (17/11823097) and the Fondation du Pélican de Mie et Pierre Hippert-Faber, under the aegis of the Fondation de Luxembourg; M.B. was supported by a European Commission Horizon 2020 Marie Skłodowska-Curie Actions individual fellowship (897408).

Conflict of interest

Mahesh S. Desai works as a consultant and an advisory board member at Theralution GmbH, Germany.

The Paper Explained

PROBLEM

There is a growing awareness that the early life period is a critical window for shaping the course of neonatal development and future health outcomes. However, little is known regarding the effects of maternal diet and microbiome composition on the interconnected establishment of the gut microbiome and host immunity in the progeny. We sought to understand the role of maternal dietary fiber intake on early life development by breeding mice colonized with a 14-member synthetic microbiota (SM), fed a fiber-deficient diet. We further investigated the effects of discrete changes in the maternal microbiome by colonizing a third breeding pair with the full SM except *Akkermansia muciniphila*, a somewhat controversial, health-associated commensal that can digest milk oligosaccharides and host mucins.

RESULTS

Pups born to dams fed a standard, fiber-rich chow showed initial colonization with *A. muciniphila*, followed by an expansion of fiber-degrading bacteria upon switching to solid food. Conversely, among pups of dams fed a fiber-free diet, *A. muciniphila* did not proliferate until after weaning,

suggesting that maternal milk factors influenced by diet shape pups' microbiome development. Pups of fiber-deprived dams expressed a significantly higher quantity of colonic tissue transcripts corresponding to defense response pathways against external antigens, and harbored lower proportions of group 2 innate lymphoid cells and Th17 cells. Pups of fiber-rich-fed mice lacking *A. muciniphila* demonstrated reduced proportions of innate and adaptive RORγt-positive immune cell subsets.

IMPACT

The link between *A. muciniphila* and RORγt-positive immune cell subsets represents an intriguing potential to alter immunity by targeting a single bacterium, however the mechanisms underlying this interaction warrant further investigation. The unexpected suppression of *Akkermansia* among pups of fiber-free fed dams during the weaning period encourages the characterization of maternal milk components that might be used to support or limit growth of certain bacteria during early life. Using a tractable gnotobiotic mouse model and custom diet, we highlight the powerful potential to manipulate the microbiome and immunity during early life, which may have important implications for prevention of modern diseases such as allergy and autoimmunity.

References

De Agüero MG, Ganal-Vonarburg SC, Fuhrer T, Rupp S, Uchimura Y, Li H, Steinert A, Heikenwalder M, Hapfelmeier S, Sauer U, *et al* (2016) The maternal microbiota drives early postnatal innate immune development. *Science (80-)* 351: 1296–1302

Ansaldo E, Farley TK & Belkaid Y (2021) Control of Immunity by the Microbiota. *Annu Rev Immunol* doi:10.1146/annurev-immunol-093019-112348 [PREPRINT]

Ansaldo E, Slayden LC, Ching KL, Koch MA, Wolf NK, Plichta DR, Brown EM, Graham DB, Xavier RJ & Moon JJ (2019) Akkermansia muciniphila induces intestinal adaptive immune responses during homeostasis. *Science (80-)* 364: 1179–1184

Arrigo A-P, Simon S, Gibert B, Kretz-Remy C, Nivon M, Czekalla A, Guillet D, Moulin M, Diaz-Latoud C & Vicart P (2007) Hsp27 (HspB1) and αB-crystallin (HspB5) as therapeutic targets. *FEBS Lett* 581: 3665–3674

Bolyen E, Rideout JR, Dillon MR, Bokulich NA, Abnet CC, Al-Ghalith GA, Alexander H, Alm EJ, Arumugam M, Asnicar F, *et al* (2019) Reproducible, interactive, scalable and extensible microbiome data science using QIIME 2. *Nat Biotechnol* doi:10.1038/s41587-019-0209-9 [PREPRINT]

Burrows K, Chiaranunt P, Ngai L & Mortha A (2020) Rapid isolation of mouse ILCs from murine intestinal tissues. In *Methods in Enzymology* pp 305–327. Elsevier

Callahan BJ, McMurdie PJ, Rosen MJ, Han AW, Johnson AJA & Holmes SP (2016) DADA2: High-resolution sample inference from Illumina amplicon data. *Nat Methods* 13: 581–583

Cheng D & Xie MZ (2021) A review of a potential and promising probiotic candidate—Akkermansia muciniphila. *J Appl Microbiol* 130: 1813–1822

Cirstea M, Radisavljevic N & Finlay BB (2018) Good bug, bad bug: breaking through microbial stereotypes. *Cell Host Microbe* 23: 10–13

Davis EC, Castagna VP, Sela DA, Hillard MA, Lindberg S, Mantis NJ, Seppo AE & Järvinen KM (2022) Gut microbiome and breast-feeding: Implications for early immune development. *J Allergy Clin Immunol* 150: 523–534

Desai MS, Seekatz AM, Koropatkin NM, Kamada N, Hickey CA, Wolter M, Pudlo NA, Kitamoto S, Terrapon N, Muller A, *et al* (2016) A Dietary Fiber-Deprived Gut Microbiota Degrades the Colonic Mucus Barrier and Enhances Pathogen Susceptibility. *Cell* 167: 1339-1353.e21

Dobin A, Davis CA, Schlesinger F, Drenkow J, Zaleski C, Jha S, Batut P, Chaisson M & Gingeras TR (2013) STAR: ultrafast universal RNA-seq aligner. *Bioinformatics* 29: 15–21

Earle KA, Billings G, Sigal M, Lichtman JS, Hansson GC, Elias JE, Amieva MR, Huang KC & Sonnenburg JL (2015) Quantitative Imaging of Gut Microbiota Spatial Organization. *Cell Host Microbe* 18: 478–488

Geerlings SY, Kostopoulos I, De Vos WM & Belzer C (2018) Akkermansia muciniphila in the human gastrointestinal tract: when, where, and how? *Microorganisms* 6: 75

Hayase E, Hayase T, Jamal MA, Miyama T, Chang C-C, Ortega MR, Ahmed SS, Karmouch JL, Sanchez CA & Brown AN (2022) Mucus-degrading Bacteroides link carbapenems to aggravated graft-versus-host disease. *Cell* 185: 3705–3719

Hepworth MR, Fung TC, Masur SH, Kelsen JR, McConnell FM, Dubrot J, Withers DR, Hugues S, Farrar MA & Reith W (2015) Group 3 innate lymphoid cells mediate intestinal selection of commensal bacteria–specific CD4+ T cells. *Science (80-)* 348: 1031–1035

Hrncir T, Stepankova R, Kozakova H, Hudcovic T & Tlaskalova-Hogenova H (2008) Gut microbiota and lipopolysaccharide content of the diet influence development of regulatory T cells: studies in germ-free mice. *BMC Immunol* 9: 1–11

Jangi S, Gandhi R, Cox LM, Li N, von Glehn F, Yan R, Patel B, Mazzola MA, Liu S, Glanz BL, *et al* (2016) Alterations of the human gut microbiome in multiple sclerosis. *Nat Commun* 7: 12015

Kalbermatter C, Fernandez Trigo N, Christensen S & Ganal-Vonarburg SC (2021) Maternal Microbiota, Early Life Colonization and Breast Milk Drive Immune Development in the Newborn. *Front Immunol* 12: 1768

Kennedy EA, King KY & Baldridge MT (2018) Mouse microbiota models: comparing germ-free mice and antibiotics treatment as tools for modifying gut bacteria. *Front Physiol* 9: 1534

Kostopoulos I, Elzinga J, Ottman N, Klievink JT, Blijenberg B, Aalvink S, Boeren S, Mank M, Knol J

& de Vos WM (2020) Akkermansia muciniphila uses human milk oligosaccharides to thrive in the early life conditions in vitro. *Sci Rep* 10: 1–17

Li S, Bostick JW, Ye J, Qiu J, Zhang B, Urban Jr JF, Avram D & Zhou L (2018) Aryl hydrocarbon receptor signaling cell intrinsically inhibits intestinal group 2 innate lymphoid cell function. *Immunity* 49: 915–928

Lin X, Tawch S, Singh A, Morgun A, Shulzhenko N & Kumar P (2021) Akkermansia muciniphila induces Th17 cells by mediating tryptophan metabolism and exacerbates experimental autoimmune encephalomyelitis (EAE). *J Immunol* 206: 105.09 LP-105.09

Liu Y, Song Y, Lin D, Lei L, Mei Y, Jin Z, Gong H, Zhu Y, Hu B & Zhang Y (2019) NCR− group 3 innate lymphoid cells orchestrate IL-23/IL-17 axis to promote hepatocellular carcinoma development. *EBioMedicine* 41: 333–344

Liu Y, Yang M, Tang L, Wang F, Huang S, Liu S, Lei Y, Wang S, Xie Z & Wang W (2022) TLR4 regulates RORγt+ regulatory T-cell responses and susceptibility to colon inflammation through interaction with Akkermansia muciniphila. *Microbiome* 10: 1–20

Love MI, Huber W & Anders S (2014) Moderated estimation of fold change and dispersion for RNA-seq data with DESeq2. *Genome Biol* 15: 550

Luna E, Parkar SG, Kirmiz N, Hartel S, Hearn E, Hossine M, Kurdian A, Mendoza C, Orr K & Padilla L (2022) Utilization efficiency of human milk oligosaccharides by human-associated Akkermansia is strain dependent. *Appl Environ Microbiol* 88: e01487-21

Macpherson AJ & Harris NL (2004) Interactions between commensal intestinal bacteria and the immune system. *Nat Rev Immunol* 4: 478–485

Martin M (2011) Cutadapt removes adapter sequences from high-throughput sequencing reads. *EMBnet J* 17: 10–12

Mirpuri J (2021) Evidence for maternal diet-mediated effects on the offspring microbiome and immunity: implications for public health initiatives. *Pediatr Res* 89: 301–306

Al Nabhani Z, Dulauroy S, Marques R, Cousu C, Al Bounny S, Déjardin F, Sparwasser T, Bérard M, Cerf-Bensussan N & Eberl G (2019) A Weaning Reaction to Microbiota Is Required for

Resistance to Immunopathologies in the Adult. *Immunity* 50: 1276–1288

Nakajima A, Vogelzang A, Maruya M, Miyajima M, Murata M, Son A, Kuwahara T, Tsuruyama T, Yamada S & Matsuura M (2018) IgA regulates the composition and metabolic function of gut microbiota by promoting symbiosis between bacteria. *J Exp Med* 215: 2019–2034

Neumann M, Steimle A, Grant ET, Wolter M, Parrish A, Willieme S, Brenner D, Martens EC & Desai MS (2021) Deprivation of dietary fiber in specific-pathogen-free mice promotes susceptibility to the intestinal mucosal pathogen Citrobacter rodentium. *Gut Microbes*

Parrish A, Boudaud M, Grant E, Willieme S, Neumann M, Wolter M, Craig S, De Sciscio A, Cosma A, Hunewald O, *et al* (2022a) Akkermansia muciniphila regulates food allergy in a diet-dependent manner. *ResearchSquare*

Parrish A, Grant E, Boudaud M, Hunewald O, Hirayama A, Ollert M, Fukuda S & Desai M (2022b) Dietary fibers boost gut microbiota-produced B vitamin pool and alter host immune landscape. *ResearchSquare*

Parrish A, Grant E, Boudaud M, Hunewald O, Hirayama A, Ollert M, Fukuda S & Desai M (2022c) Dietary fibers boost gut microbiota-produced B vitamin pool and alter host immune landscape. *ResearchSquare*: [PREPRINT]

Pereira GV, Boudaud M, Wolter M, Alexander C, De Sciscio A, Grant E, Trindade BC, Singh S, Campbell A & Pudlo N (2022) Unravelling specific diet and gut microbial contributions to inflammatory bowel disease. *bioRxiv*

Qiu J, Heller JJ, Guo X, Zong-ming EC, Fish K, Fu Y-X & Zhou L (2012) The aryl hydrocarbon receptor regulates gut immunity through modulation of innate lymphoid cells. *Immunity* 36: 92–104

Quast C, Pruesse E, Yilmaz P, Gerken J, Schweer T, Yarza P, Peplies J & Glöckner FO (2013) The SILVA ribosomal RNA gene database project: Improved data processing and web-based tools. *Nucleic Acids Res*

Robertson RC, Manges AR, Finlay BB & Prendergast AJ (2019) The human microbiome and child growth–first 1000 days and beyond. *Trends Microbiol* 27: 131–147

Sonnenburg ED, Smits SA, Tikhonov M, Higginbottom SK, Wingreen NS & Sonnenburg JL (2016) Diet-induced extinctions in the gut microbiota compound over generations. *Nature* 529: 212–215

Spidlen J, Breuer K, Rosenberg C, Kotecha N & Brinkman RR (2012) FlowRepository: A resource of annotated flow cytometry datasets associated with peer-reviewed publications. *Cytom Part A*

Steimle A, De Sciscio A, Neumann M, Grant ET, Pereira G V., Ohno H, Martens EC & Desai MS (2021) Constructing a gnotobiotic mouse model with a synthetic human gut microbiome to study host–microbe cross talk. *STAR Protoc* 2

Szanto I, Rubbia- Brandt L, Kiss P, Steger K, Banfi B, Kovari E, Herrmann F, Hadengue A & Krause K (2005) Expression of NOX1, a superoxide- generating NADPH oxidase, in colon cancer and inflammatory bowel disease. *J Pathol A J Pathol Soc Gt Britain Irel* 207: 164–176

Wells JM, Gao Y, de Groot N, Vonk MM, Ulfman L & van Neerven RJJ (2022) Babies, Bugs, and Barriers: Dietary Modulation of Intestinal Barrier Function in Early Life. *Annu Rev Nutr* 42

Xie Y-H, Gao Q-Y, Cai G-X, Sun X-M, Zou T-H, Chen H-M, Yu S-Y, Qiu Y-W, Gu W-Q & Chen X-Y (2017) Fecal Clostridium symbiosum for noninvasive detection of early and advanced colorectal cancer: test and validation studies. *EBioMedicine* 25: 32–40

Yoon HS, Cho CH, Yun MS, Jang SJ, You HJ, Kim J, Han D, Cha KH, Moon SH & Lee K (2021) Akkermansia muciniphila secretes a glucagon-like peptide-1-inducing protein that improves glucose homeostasis and ameliorates metabolic disease in mice. *Nat Microbiol* 6: 563–573

Yu G, Wang L-G, Han Y & He Q-Y (2012) clusterProfiler: an R package for comparing biological themes among gene clusters. *Omi a J Integr Biol* 16: 284–287

Zheng W, Zhao W, Wu M, Song X, Caro F, Sun X, Gazzaniga F, Stefanetti G, Oh S & Mekalanos JJ (2020) Microbiota-targeted maternal antibodies protect neonates from enteric infection. *Nature* 577: 543–548

Zhu H, Wang G, Zhu H & Xu A (2021) ITGA5 is a prognostic biomarker and correlated with immune infiltration in gastrointestinal tumors. *BMC Cancer* 21: 1–14

Figure legends

Figure 1. Delayed expansion of *Akkermansia* among offspring of fiber-deprived dams.

A. Schematic representation of the study design.

B. Stream plot showing the relative abundance of the 14 bacterial strains in the colons of pups born to 14SM FF-fed mice, 14SM FR-fed mice and 13SM FR-fed dams. Distal colon contents were analyzed by qPCR using primers specific to each bacteria and present once per genome.

C. Line plots of the mean relative abundances and SD of each bacterial strain from ages 10 to 30 days. Data were normally distributed according to the Kolmogorov-Smirnov test and statistical significance compared to the 14SM FR control at each time point was calculated by two-way ANOVA with false-discovery adjustment using the Benjamini and Hochberg method. The adjusted *p* values are indicated for 14SM FF vs 14SM FR (red) and 13SM FR vs 14SM FR (orange).

Figure 2. Maternal diet alters colonic transcriptome of offspring at age 15 days.

A. Table depicting counts of genes with differential transcription groups after filtering reads not present at least once across all samples (top) and differentially enriched pathways between groups according to the Gene Ontologies (GO) terms for all processes (bottom).

B. Volcano plot showing gene abbreviations for transcripts that were significantly enriched in 14SM FF or 14SM FR after correction for multiple comparisons using DESeq2.

C. Network plots displaying pathways for biological processes and their associated genes that were differentially represented in pups born to 14SM FF vs 14SM FR dams. Top five up- and down-regulated pathways for biological processes are shown; all pathways can be found in **Table S8**.

D. mRNA expression of *Ifng*, *Tnfa*, *Il17f*, and *Il22*. Transcription levels were normalized by *Hprt*, which was the most stable among the three housekeeping genes tested (*Hprt, Hsp90, Gapdh)*. Longitudinal data of mean ± SEM is shown for 14SM FF, 14SM FR, and 13SM FR pups at age 10-20 days (circles) with statistical significance calculated using two-way ANOVA factored on group and time point compared to the 14SM FR control. In addition to the 14SM FF, 14SM FR,

and 13SM FR groups, we report transcript levels for pups born to germfree (GF) FF or FR dams at age 15 days (squares) with statistical significance based on a one-way ANOVA with false-discovery adjustment using the Benjamini and Hochberg method. Outliers removed using ROUT method with Q = 1%.

Figure 3. Maternal diet and microbiome shapes innate and adaptive neonatal immune cell populations.

A. For 14SM and GF FF- and FR-fed mice at age 15 days, the proportion of cytotoxic natural killer (cNK), innate lymphoid cell (ILC) type 1, ILC type 2, ILC type 3, natural cytotoxicity receptor (NCR) positive ILC3, and NCR negative ILC3 populations among CD45+ cells.
B. For 14SM and GF FF- and FR-fed mice at age 15 days, the proportion of CD8+ T cells, CD4+ T cells, Tregs (total FoxP3+), Th1 cells (Tbet+), Th2 (GATA3+), and Th17 (RORgt+) populations among CD45+ cells.
C. For 13SM, 14SM, and GF FR-fed at age 15 days, the proportion of cNK, ILC1, ILC2, ILC3, NCR+ ILC3, and NCR- ILC3 populations among CD45+ cells.
D. For 13SM, 14SM, and GF FR-fed at age 15 days, the proportion of CD8+ T cells, CD4+ T cells, Tregs , Th1, Th2, and Th17 populations among CD45+ cells.

Statistical significance is based on a two-way ANOVA (A-B) or one-way ANOVA (C-D) with false-discovery adjustment using the Benjamini and Hochberg method.

Figure 4. Summary of key transcriptional, cellular, and microbial shifts among pups of 14SM fiber-deprived dams. Maternal milk components (immunoglobulins, altered milk glycan structures) among fiber-deprived dams are predicted to inhibit the establishment of mucin-degrading bacteria in the suckling period, after which this functional group rapidly expands, following a pattern inverse to pups of FR-fed dams. These microbial changes are accompanied by an array of host changes characterized by transcripts involved in epithelial development and innate defense signaling as well as differential priming of key immune cell subsets.

Supplementary Information

Figure S1.

A. PCA plot of samples analyzed by RNA sequencing datasets. B.

B. Volcano plot showing transcripts that were significantly enriched in 14SM FR or 13SM FR after correction for multiple comparisons using DESeq2.

C. mRNA expression of *Il12p40* and *Il23*. Transcription levels were normalized by *Hprt*, which was the most stable among the three housekeeping genes tested (*Hprt, Hsp90, Gapdh)*. Longitudinal data of mean ± SEM is shown for 14SM FF, 14SM FR, and 13SM FR pups at age 10-20 days (circles) with statistical significance calculated using a two-way ANOVA factored on group and time point compared to the 14SM FR control. For *Il23*, we also report transcript levels for pups born to germfree (GF) FF or FR dams at age 15 days (squares) with statistical significance based on a one-way ANOVA with false-discovery adjustment using the Benjamini and Hochberg method. Outliers removed using ROUT method with Q = 1%.

Figure S2. Representative gating strategy for flow cytometry analysis.

Table S1. Primers for RT-qPCR against colonic cDNA transcript library.

Table S2. Absolute abundances of synthetic microbiota (SM) members among parent mice.

Table S3. Absolute abundances of synthetic microbiota (SM) members among individual pups.

Table S4. 16S rRNA gene sequencing to rule out contamination with non-14SM bacteria.

Table S5. Count table of transcripts mapping to genes by ENSEMBL identifier. Asterisk (*) indicates samples identified as outliers by PCA plotting.

Table S6. Differential enrichment analysis using DESeq2 for 14SM fiber-free and 14SM fiber-rich contrasts.

Table S7. Differential enrichment analysis using DESeq2 for 14SM fiber-rich and 13SM fiber-rich contrasts.

Table S8. Pathway level differential enrichment analysis using clusterProfiler (all processes) for 14SM fiber-free and 14SM fiber-rich contrasts.

Fig1

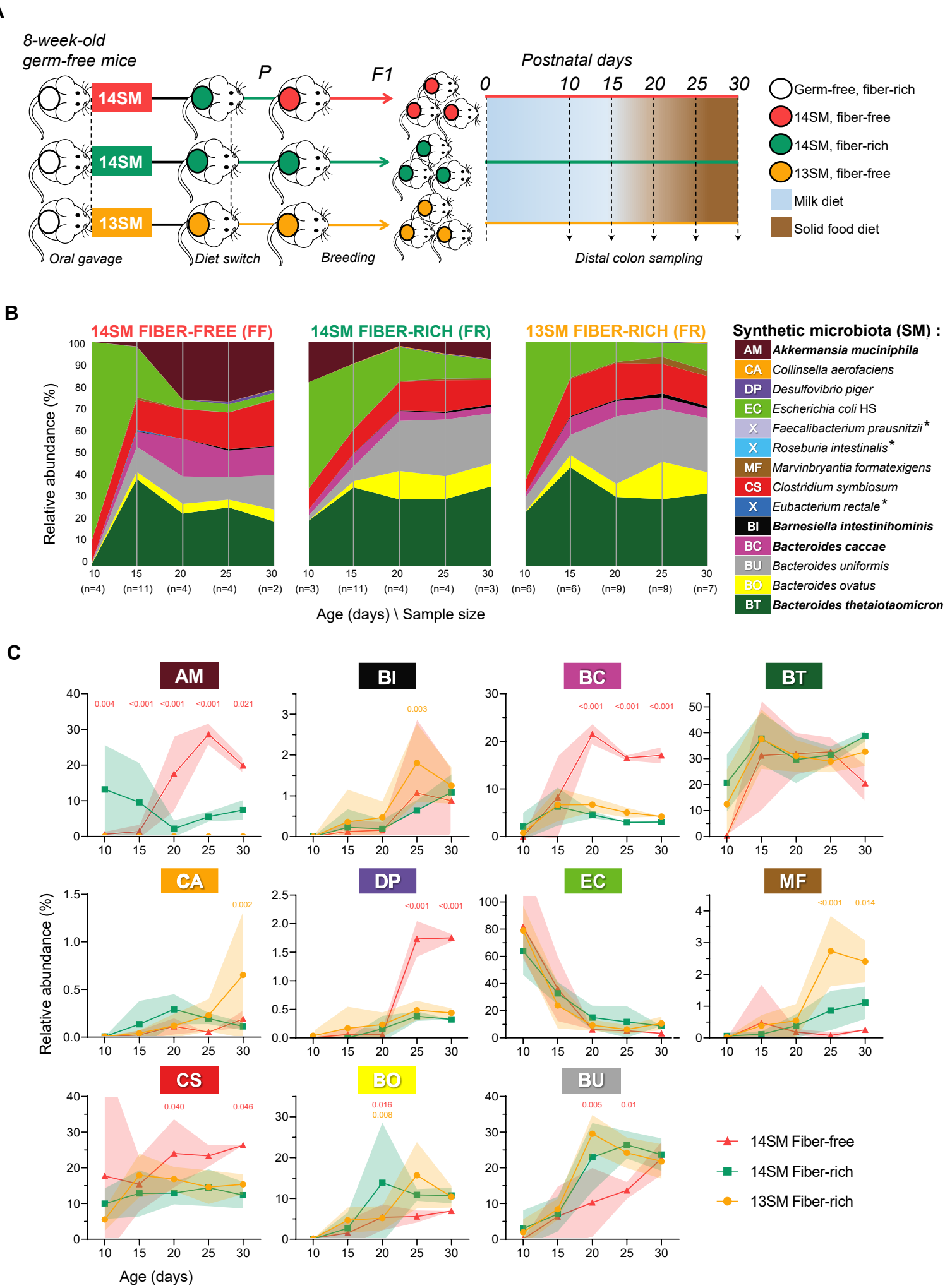
A
8-week-old germ-free mice
14SM
14SM
13SM
P
F1
Postnatal days
0
10
15
20
25
30
Germ-free, fiber-rich
14SM, fiber-free
14SM, fiber-rich
13SM, fiber-free
Milk diet
Solid food diet
Oral gavage
Diet switch
Breeding
Distal colon sampling
B
14SM FIBER-FREE (FF)
14SM FIBER-RICH (FR)
13SM FIBER-RICH (FR)
Relative abundance (%)
Age (days) \ Sample size
Synthetic microbiota (SM) :
AM Akkermansia muciniphila
CA Collinsella aerofaciens
DP Desulfovibrio piger
EC Escherichia coli HS
X Faecalibacterium prausnitzii*
X Roseburia intestinalis*
MF Marvinbryantia formatexigens
CS Clostridium symbiosum
X Eubacterium rectale*
BI Barnesiella intestinihominis
BC Bacteroides caccae
BU Bacteroides uniformis
BO Bacteroides ovatus
BT Bacteroides thetaiotaomicron
C
AM
BI
BC
BT
CA
DP
EC
MF
CS
BO
BU
Relative abundance (%)
Age (days)
14SM Fiber-free
14SM Fiber-rich
13SM Fiber-rich

Fig2

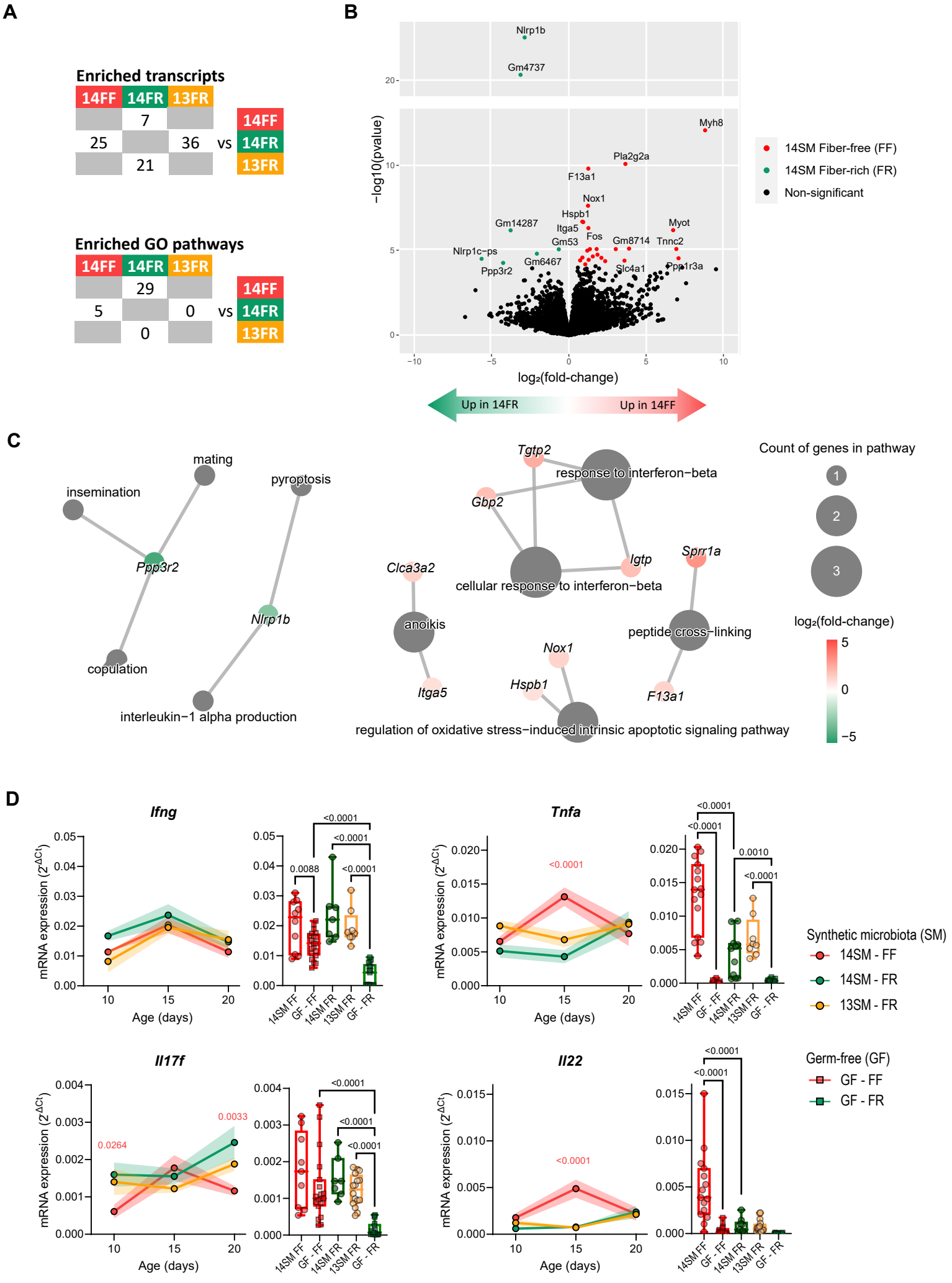
A
Enriched transcripts
14FF 14FR 13FR
7
25 36 vs 14FF 14FR 13FR
21
Enriched GO pathways
14FF 14FR 13FR
29
5 0 vs 14FF 14FR 13FR
0
B
Nlrp1b
Gm4737
Myh8
Pla2g2a
F13a1
Nox1
Hspb1
Itga5
Fos
Gm53
Gm14287
Myot
Gm8714
Tnnc2
Nlrp1c−ps
Gm6467
Ppp3r2
Slc4a1
Ppp1r3a
−log10(pvalue)
log2(fold-change)
14SM Fiber-free (FF)
14SM Fiber-rich (FR)
Non-significant
Up in 14FR
Up in 14FF
C
mating
insemination
pyroptosis
Ppp3r2
Nlrp1b
copulation
interleukin−1 alpha production
Tgtp2
response to interferon−beta
Gbp2
Igtp
Sprr1a
Clca3a2
cellular response to interferon−beta
anoikis
peptide cross−linking
Nox1
Hspb1
Itga5
F13a1
regulation of oxidative stress−induced intrinsic apoptotic signaling pathway
Count of genes in pathway
1
2
3
log2(fold-change)
5
0
−5
D
Ifng
Tnfa
Il17f
Il22
mRNA expression (2^ΔCt)
Age (days)
<0.0001
0.0088
0.0010
0.0264
0.0033
14SM FF
GF - FF
14SM FR
13SM FR
GF - FR
Synthetic microbiota (SM)
14SM - FF
14SM - FR
13SM - FR
Germ-free (GF)
GF - FF
GF - FR

Fig3

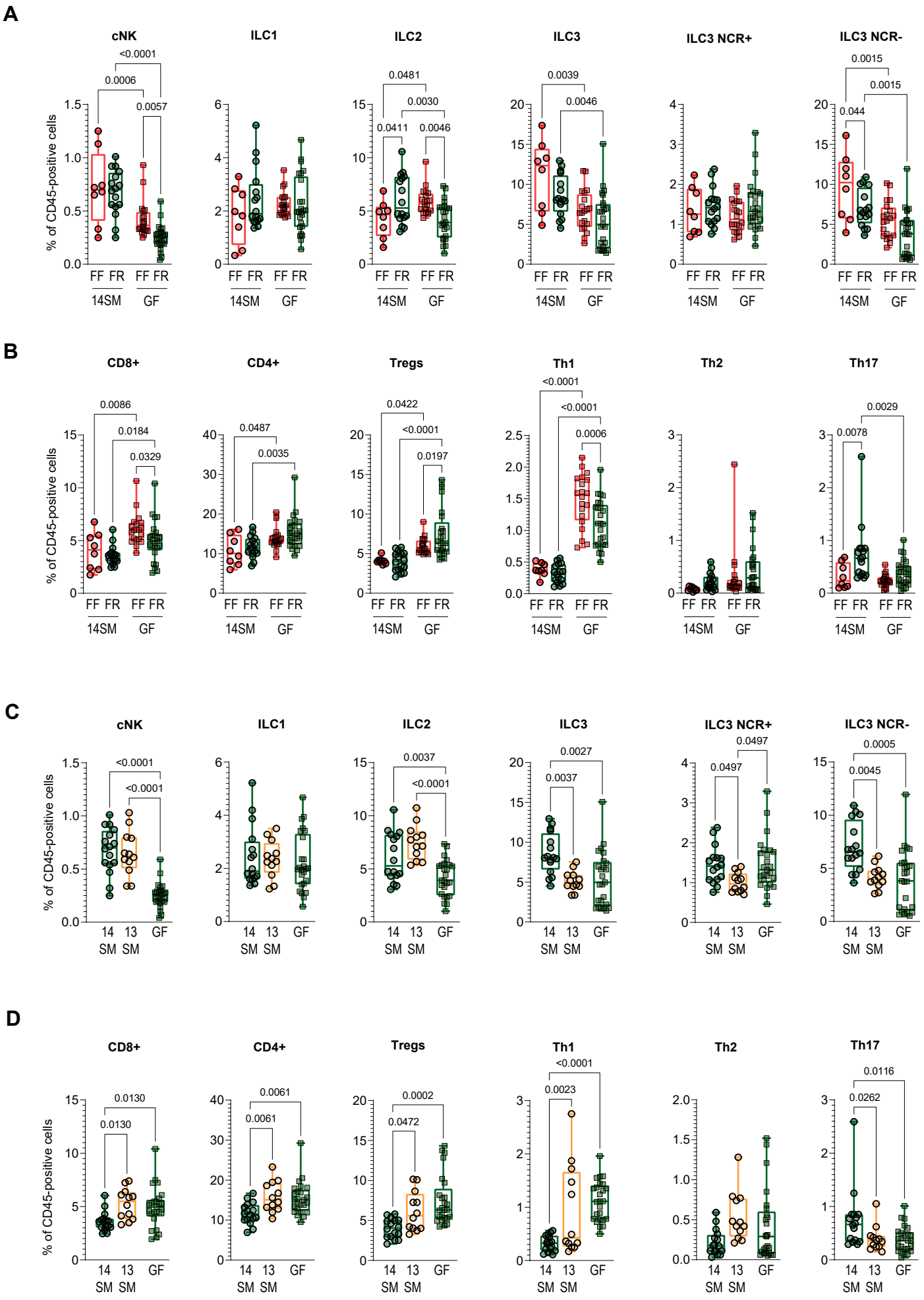
A
cNK
ILC1
ILC2
ILC3
ILC3 NCR+
ILC3 NCR-
% of CD45-positive cells
FF FR FF FR
14SM GF
B
CD8+
CD4+
Tregs
Th1
Th2
Th17
C
14 SM 13 SM GF
D

Fig4

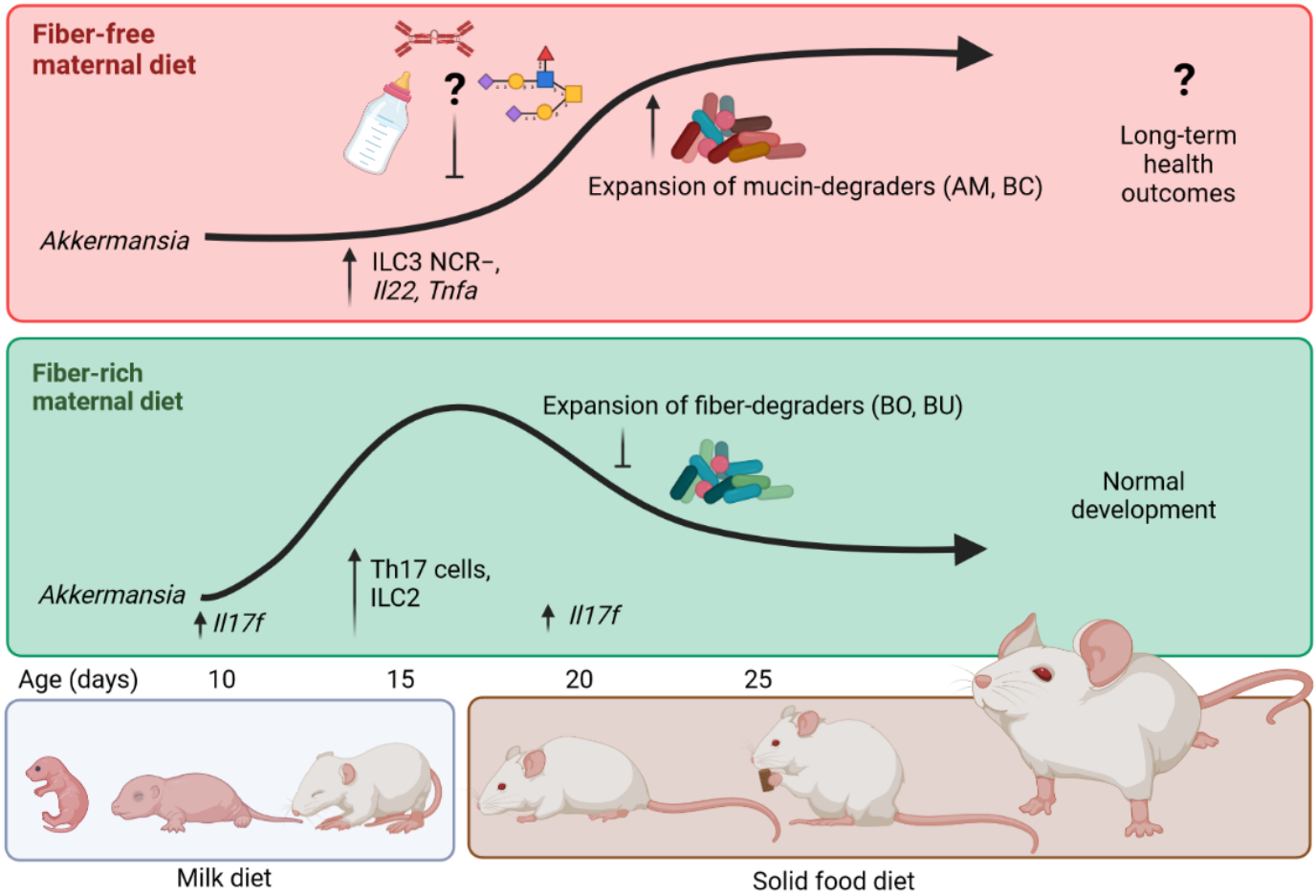
Fiber-free maternal diet
?
Expansion of mucin-degraders (AM, BC)
?
Long-term health outcomes
Akkermansia
ILC3 NCR−, Il22, Tnfa
Fiber-rich maternal diet
Expansion of fiber-degraders (BO, BU)
Normal development
Akkermansia
Il17f
Th17 cells, ILC2
Il17f
Age (days)
10
15
20
25
Milk diet
Solid food diet

FigS1

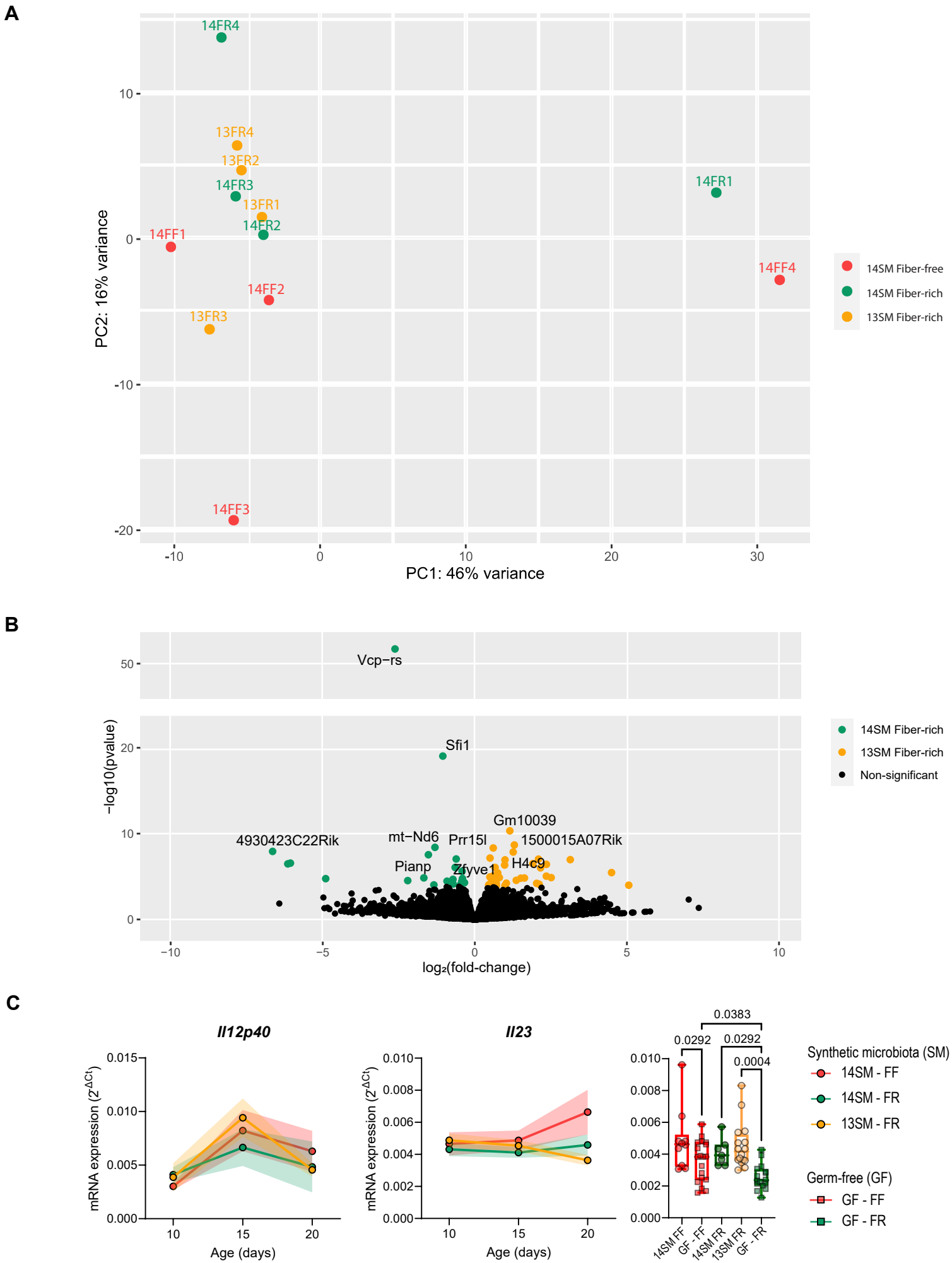
A
14FR4
13FR4
13FR2
14FR3
13FR1
14FR2
14FF1
14FF2
13FR3
14FF3
14FR1
14FF4
PC2: 16% variance
PC1: 46% variance
14SM Fiber-free
14SM Fiber-rich
13SM Fiber-rich
B
Vcp−rs
Sfi1
Gm10039
4930423C22Rik
mt−Nd6
Prr15l
1500015A07Rik
Pianp
Zfyve1
H4c9
−log10(pvalue)
log2(fold-change)
14SM Fiber-rich
13SM Fiber-rich
Non-significant
C
Il12p40
Il23
mRNA expression (2^ΔCt)
Age (days)
0.0383
0.0292
0.0292
0.0004
14SM FF
GF - FF
14SM FR
13SM FR
GF - FR
Synthetic microbiota (SM)
14SM - FF
14SM - FR
13SM - FR
Germ-free (GF)
GF - FF
GF - FR

FigS2

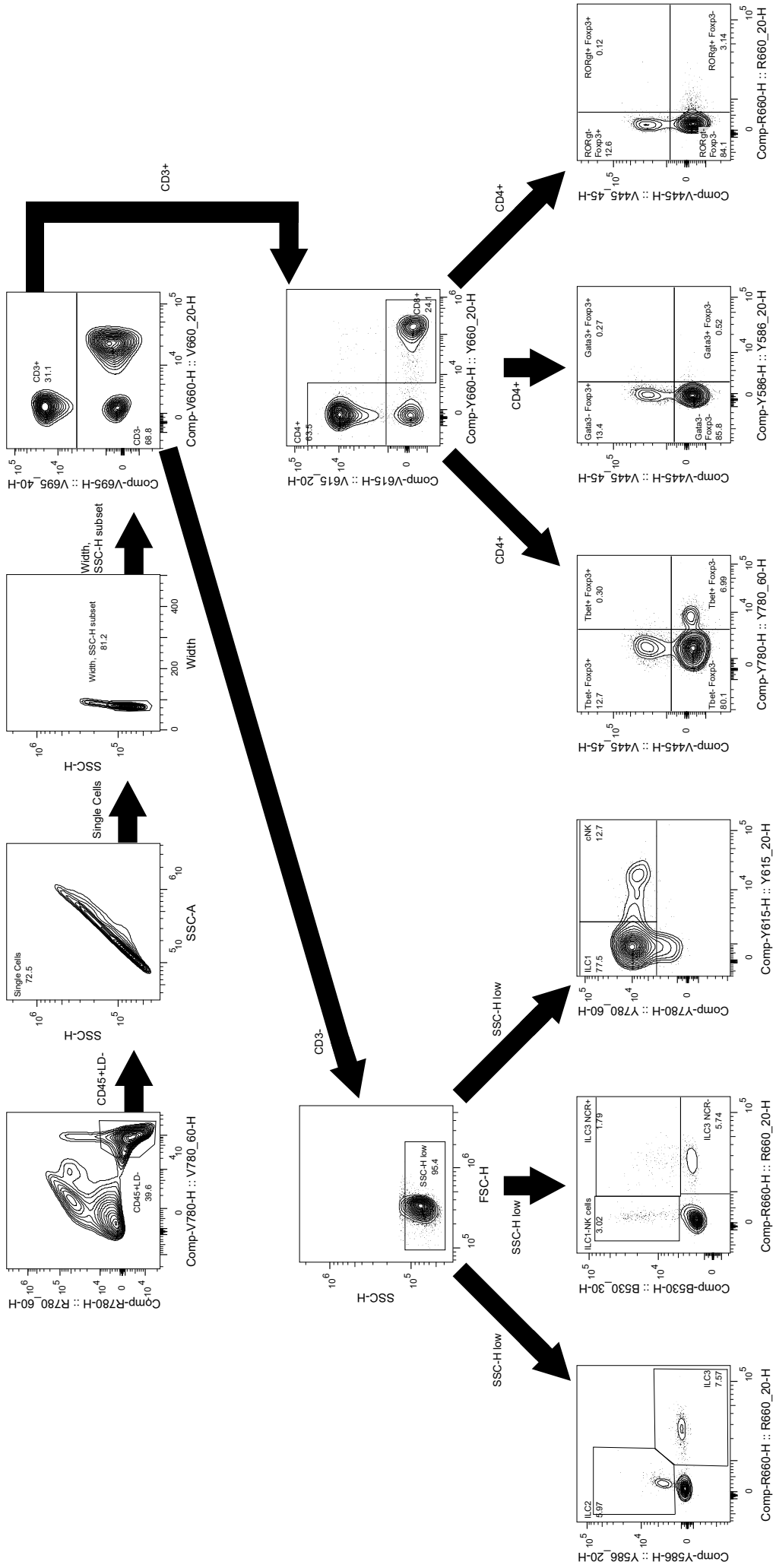
CD45+LD-
39.6
Comp-V780-H :: V780_60-H
Comp-R780-H :: R780_60-H
Single Cells
72.5
SSC-A
SSC-H
Single Cells
Width, SSC-H subset
81.2
Width
SSC-H
Width, SSC-H subset
CD3+
31.1
CD3-
68.8
Comp-V660-H :: V660_20-H
Comp-V695-H :: V695_40-H
CD3+
CD3-
SSC-H low
95.4
FSC-H
SSC-H
CD4+
63.5
CD8+
24.1
Comp-Y660-H :: Y660_20-H
Comp-V615-H :: V615_20-H
CD4+
CD4+
CD4+
SSC-H low
SSC-H low
SSC-H low
ILC1
77.5
cNK
12.7
Comp-Y780-H :: Y780_60-H
Comp-Y615-H :: Y615_20-H
ILC1-NK cells
3.02
ILC3 NCR+
1.79
ILC3 NCR-
5.74
Comp-R660-H :: R660_20-H
Comp-B530-H :: B530_30-H
ILC2
5.97
ILC3
7.57
Comp-R660-H :: R660_20-H
Comp-Y586-H :: Y586_20-H
Tbet- Foxp3+
12.7
Tbet+ Foxp3+
0.30
Tbet- Foxp3-
80.1
Tbet+ Foxp3-
6.99
Comp-Y780-H :: Y780_60-H
Comp-V445-H :: V445_45-H
Gata3- Foxp3+
13.4
Gata3+ Foxp3+
0.27
Gata3- Foxp3-
85.8
Gata3+ Foxp3-
0.52
Comp-Y586-H :: Y586_20-H
Comp-V445-H :: V445_45-H
RORgt- Foxp3+
12.6
RORgt+ Foxp3+
0.12
RORgt- Foxp3-
84.1
RORgt+ Foxp3-
3.14
Comp-R660-H :: R660_20-H
Comp-V445-H :: V445_45-H